EXPERIMENTAL PAPERS

Topography of the Ganglion Retinal Layer and Retinal Resolution in the Rough-Toothed Dolphin *Steno bredanensis* (Cetacea: Delphinidae)

A. M. Mass[a],* and A. Ya. Supin[a]

[a] *Institute of Ecology and Evolution, Russian Academy of Sciences, Moscow, Russia*
*e-mail: alla-mass@mail.ru

Abstract—Morphological investigation of the retinal ganglion layer in the rough-toothed dolphin *Steno bredanensis* was performed using the retinal wholemount technique. Mapping of the density of ganglion cells revealed two areas of their concentration: in the nasal (544 cells/mm^2) and temporal (594 cells/mm^2) quadrants. Ganglion cell diameters ranged from 12 to 50 μm, with mean values varying from 20 to 29 μm in different areas. The obtained cell densities corresponded to a retinal resolution of 11'.

INTRODUCTION

Studies of the visual system in cetaceans revealed peculiarities of their retinal organization that are unusual for most terrestrial mammals. This primarily concerns the areas with high concentration of ganglion cells responsible for retinal resolution. The shape and location of these areas may differ in different cetacean species, depending on their habitat conditions and systematic position [1].

Data on the topography of ganglion cells, including those on the shape and localization of areas with increased ganglion cell concentration, were obtained on retinal wholemount preparations. This technique proved to be useful also for studying vision in hard-to-reach species of marine mammals for which the use of other methods (electrophysiological, behavioral) is either difficult or impracticable. This approach enabled data on the organization of visual fields to be obtained in some cetacean species [2–7].

The organization of visual fields is highly variable in different cetacean species. This difference is largely dependent on optical properties of a habitat. In members of several families of toothed whales (Odontoceti) [2–6] and some baleen whales (Mysticeti) [7, 8] that inhabit highly transparent waters, there are two high-resolution areas: in the nasal and temporal quadrants. A fundamentally different arrangement of the visual field was found in the Amazon river dolphin *Inia geoffrensis* (Iniidae) inhabiting river waters with low transparency. In addition to the low density of ganglion cell, they were found to have a single area of increased resolution located in the dorsal

part of the visual field [9].

In view of the data on the dependence of visual fields on the properties of whale habitats, it is of interest to address the organization of visual fields in those species whose mode of life combines being in waters both with high and low transparency. One of such species is the rough-toothed dolphin *Steno bredanensis* Cuvier in Lesson, 1828 (Delphinidae, Odontoceti). These cetaceans of a relatively small size occur both in shallow coastal and deep ocean waters of tropical and subtropical zones [10]. The visual system of the rough-toothed dolphin is essentially unstudied. There is a single study of its cornea (visual ceratometric monitoring [11]). In the literature, there is no information on the general eye morphology, retinal organization, or the visual system's spatial resolution in this species. Hence, it is unknown to which extent the visual field organization in the rough-toothed dolphin is similar to that in toothed whales inhabiting waters either with low or high transparency. The solution of this issue may contribute to understanding to what extent the organization of the visual fields in cetaceans depends on the systematic position of the species and to what extent on the habitat conditions.

This work aimed to explore the morphology and geometrical parameters of the eye, retinal topography and visual field organization, as well as retinal resolution, in the rough-toothed dolphin *S. bredanensis*.

MATERIALS AND METHODS

Materials. The study was carried out on two eyes taken from one adult rough-toothed dolphin *Steno bredanensis* with a body length of 130 cm, which was found in 2002 on the beach in the South China Sea during the joint Russian-Vietnamese expedition. The animal was identified as a rough-toothed dolphin *S. bredanensis* Cuvier in Lesson. Before the study, the material was stored in 10% buffered formalin that was changed once a year.

Material preparation. Both eyes were used to prepare wholemount preparations. To do this, eyes were fixed in 10% buffered formalin. Such a fixation is most suitable for preparing large-area retinal wholemounts.

Before extracting the retina, external measurements of the eye were made to obtain the diameter and axial length of the eyeball, as well as the size of the retina and pupil. To extract the retina, the cornea, lens and vitreous body were removed, thus exposing the eyecup. The lens and the inner diameter of the eyecup were measured. The retina was notched twice to distinguish between its dorsal and ventral poles and then separated from the pigment epithelium. On the extracted retina, several radial cuts were made to mount it flat on the glass slide. The retina was mounted with the ganglion layer upward and then air dried. The resultant wholemount was stained with 0.1% cresyl violet by Nissl method. The degree of staining was controlled visually, and the process was stopped as soon as the outermost ganglion cell layer was stained. Thereby, all the superficially lying ganglion cells were stained, providing the important prerequisite for their count. The stained wholemount was dehydrated in an ascending series of ethanol, cleared in xylene, and embedded in Permount (Electron Microscopy Sciences, USA). Although a slight shrinkage of the preparation was observed along the margins of the cuts, the fixation quality throughout the rest of the wholemount did not suffer.

Wholemount microscopic examination. The distribution pattern of ganglion cells across the retinal wholemount preparation was examined using an Olympus BX41 microscope (Japan). The depth of the objective lens focus was equal to the depth of the ganglion layer. Ganglion cells were counted systematically within this layer across the entire retinal surface every 1 mm in squares of 0.5×0.5 mm; the boundaries of the squares were set by the eyepiece graticule (ocular $\times 10$). The coordinates of the areas within which cells were counted were preset by the coordinates of the microscopic stage. As a rule, in 0.25-mm^2 squares, there were counted no less than 20 cells, while in the areas of high cell density—up to 150 cells, which was considered sufficient for mapping at a satisfactory resolution. The resultant values of the number of cells per 0.25-mm^2 squares were recalculated into the cell density (the number of cells per 1 mm^2), and to reduce the data scatter, moving averaging was performed in the blocks of 2×2 mm. Using these results, maps of ganglion cell density were com-

posed. For mapping, we used a custom-made program under a LabVIEW software shell (National Instruments, USA).

Maps of ganglion cell distribution were also used to calculate the total number of cells and the retinal area. The total number of cells was determined as the number of cells in all 1-mm^2 squares. The retinal area was determined as the number of 1-mm^2 squares.

Cell sizes were measured in retinal areas with different cell densities: with high density (nasal and temporal) and low density (dorsal and ventral quadrants). Measurements were carried out on digital microphotographs taken from the selected retinal wholemount areas (Moticam 2300 camera, China) using the Motic Image Plus 2.0 software (Hong Kong). The areas of cell profiles were measured, and the resultant values were recalculated into the diameter of a circle, which was taken as the size of the cell body.

In more detail, the techniques for preparing and examining of retinal wholemounts are described in a number of publications [12−14], including for aquatic mammals [15, 16].

RESULTS

Dimensions of the eye. The eye of the rough-toothed dolphin had properties typical of many species of marine cetaceans studied up to now. The eyeball was cone-shaped due to well-developed retractor muscles attached to the posterior ocular segment of the eye. The eyeball was slightly flattened in the dorso-ventral direction, with the horizontal diameter (26.5 mm) being larger than the vertical (24.5 mm). The lens was flattened a little in the axial direction, with the diameter being 8 mm and the axial length—7 mm. The pupil (6.5 × 3.4 mm) was elongated horizontally. The upper edge of the iris formed the U-shaped operculum. The well-developed bright blue-green tapetum covered the entire eyecup except the small ventral dark-pigmented area. The sclera was thick, the anterior chamber was small. The slightly oval-shaped cornea was flattened in the dorso-ventral direction: its horizontal diameter was 16.5 mm, vertical—15 mm. The optic nerve outlet was situated 1–2 mm dorsally to the eyeball axis. The diameter of the optic nerve was 3 mm.

Characteristics of ganglion cells. To identify ganglion cells, we employed the criteria proposed in studies carried out on other species of terrestrial [12, 14, 17−20] and marine [5, 15, 16] mammals. In accordance with these criteria, multipolar cells in the superficial retinal layer were considered ganglion cells provided they had the following characteristics: (i) the size is not less than 10 μm, (ii) cytoplasm with intensely stained granules of the Nissl substance, (iii) well discernible light nucleus with a distinct nucleolus (Fig. 1). The nucleus might be located either centrally or eccentrically.

The shape of ganglion cells varied. Most of cells were round or oval, sometimes with distinct processes. Spindle-like cells also occured. In very large neurons, one or two processes extending from the soma were visible.

In addition to typical ganglion cells, the cell layer contained small cells with the large opaque nucleus and narrow cytoplasmic rim around it. These cells reside at the same levels as ganglion neurons and, according to the criteria described previously [14, 16, 17−20], were considered amacrine neurons; they were excluded from further consideration.

The characteristic feature of the retinal ganglion cell layer in the *S. bredanensis* was a low density of ganglion cells: the layer was composed of sparse neurons with large cell-to-cell distances. These distances were particularly large in the areas of low cell density, while in the areas of high density, the distances were smaller, as seen in fragments of wholemounts presented in Fig. 1.

Topography of ganglion cell distribution. As seen in microphotographs of the ganglion layer (Figs. 1a, 1b), the density of ganglion cells was dissimilar in different retinal areas. Quantitative data on the topographic distribution of ganglion cells were obtained on both available wholemounts arbitrarily defined below as no. 1 (left eye) and no. 2 (right eye).

Areas of both preparations were 665 and 780 mm^2 (difference, 17%), on average 722 mm^2. The total number of ganglion cells per retina was 137 thousand (no. 1) and 147 thousand (no. 2) (difference, 7%), on average 142 thousand.

Ganglion cells were counted across the entire wholemount area. If no cells were found in some
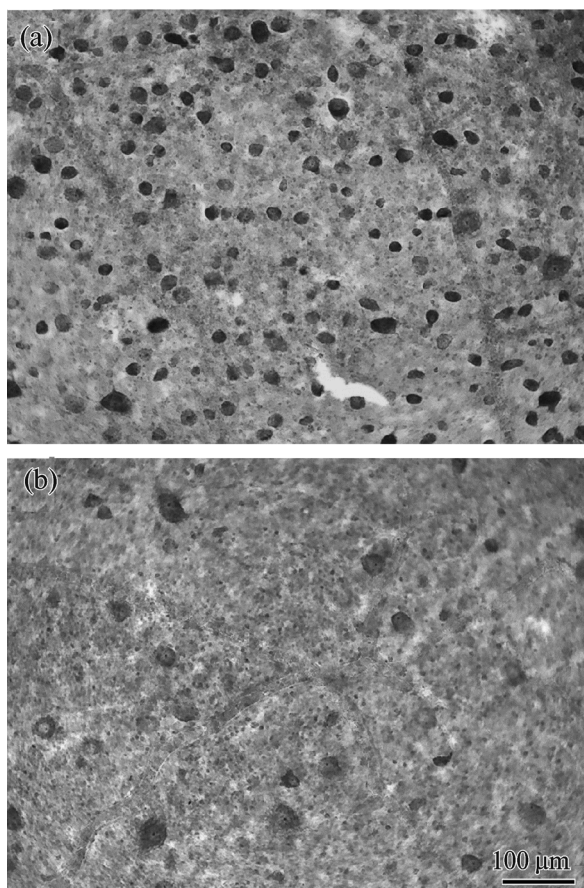
Fig. 1. Microphotographs of the ganglion cell layer. (a) Area of high concentration of ganglion cells. (b) Area of low distribution density of ganglion cells.

square (which was a very rare instance), this was mapped as 0. At the margins of the radial cuts, where there was a slight dehydration-induced tissue shrinkage, no increased density of ganglion cells was observed. This instance was interpreted as an indication that the shrinkage had no appreciable influence on cell density mapping.

Mapping of the ganglion cell distribution in both wholemounts (Fig. 2) revealed that the retinae contained two zones of increased cell density looking as two elongated oval-shaped areas. In both wholemounts, the areas of increased density were alike in their location, size, shape and orientation. One of them was situated in the temporal quadrant, another — in the nasal quadrant of the retina. Areas of maximum cell density lied closer to the periphery at a distance of 12–13 mm from the optic disc. Maximum densities in both areas differed insignificantly and were, respectively, 544 and 616 cells/mm^2 (difference, 13%) in the whol-

emount no. 1 and 543 and 571 cells/mm^2 (difference, 5%) in the wholemount no. 2. The means of density maxima for two wholemounts were 544 and 594 cells/mm^2, respectively, in the nasal and temporal quadrants.

The distribution of ganglion cell densities in both wholemounts is demonstrated by the profiles of density distribution along the line passing through both areas of increased density and the center of the retina (Fig. 3). At such a representation, two peaks of increased density can be seen in the temporal and nasal quadrants, as well as a significant drop in the density in between.

Sizes of ganglion cells. In the wholemount no. 1, sizes of 440 cell bodies in three retinal areas with different distribution density of ganglion cells were measured. The results of measurements are presented in Fig. 4: (a)—for the temporal high-density area, (b)—for nasal high-density area (in both areas, density exceeds 500 cells/mm^2), and (c)—for low-density area at the periphery of the nasal quadrant (density around 100 cells/mm^2). Cell sizes ranged from 12 to 50 μm. In the temporal and nasal regions, the size of the cell body varied from 12 to 28 μm, in the low-density area — from 14 to 50 μm. Mean sizes in the temporal and nasal areas were almost equal: 20 and 21 μm, respectively. In the low-density area, the mean cell size was larger: 29 μm.

DISCUSSION

Sizes of ganglion cells. The retina of the rough-toothed dolphin is characterized by large, sparsely spaced ganglion cells. Large ganglion cells were described previously in several whale and dolphin species [4, 6–8, 21, 22]. Most of them were shown to have diameters of their bodies ranging from 12 to 35 μm, while individual neurons reached 60–75 μm and even more. In the retina of the killer whale *Orcinus orca*, there were found giant ganglion cells ranging from 80 to 100 μm [5]. Thus, sizes of the bulk of ganglion neurons in the rough-toothed dolphin are basically alike those in the retina of the majority of other cetaceans studied by now, although cells larger than 50 μm were not found in the rough-toothed dolphin.

The number of ganglion cells. The total number of cells in the retina of the rough-toothed dolphin
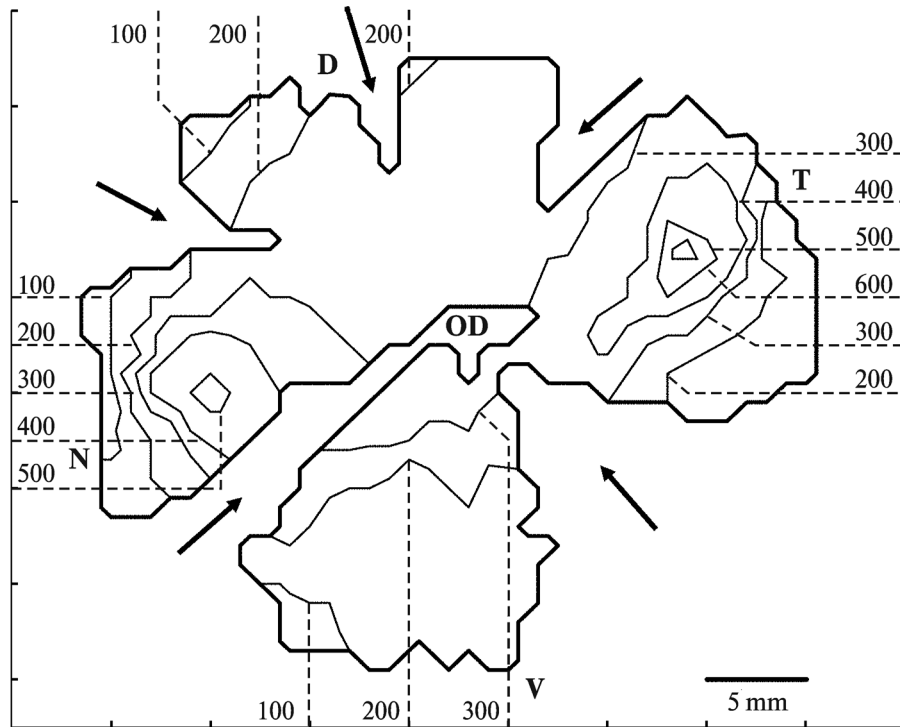
Fig. 2. Map of ganglion cell density in the retinal wholemount of the rough-toothed dolphin (left eye). Cell densities are marked by equilevel lines the values of which are indicated at map sides. D, V, N, T—dorsal, ventral, nasal and temporal retinal poles, respectively; OD—optic disc. Arrows indicate radial cuts made to flatten the retina on a slide.
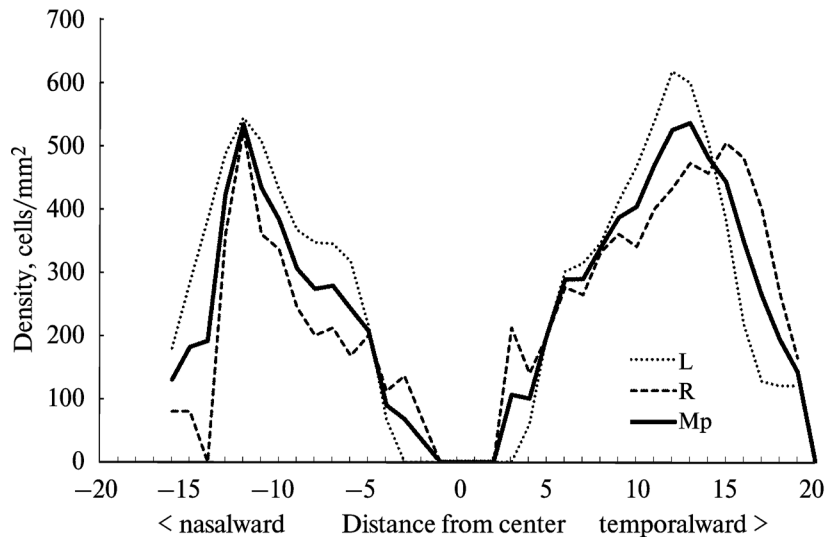

Fig. 3. Distribution of ganglion cell density along the line passing through the areas of high density and the center of the wholemount. L—Left eye, R—right eye, Mp—means for two perparations.

(142 thousand) is comparable to that in other cetaceans: 122 thousand in the beluga whale *Delphinapterus leucas* [4, 6]; 112−199 thousand in *O. orca* [5] and the false killer whale *Pseudorca crassidens* [6]; 220 thousand in the bottlenose dolphin *T. truncatus* [2]. These values are close to the data on the number of fibers in the killer whale optic nerve—137 thousand [23] and bottlenose dolphin—from 157 to 185 thousand [22, 24, 25].

Distribution of ganglion cells. The rough-toothed dolphin is characterized by a relatively low, compared to terrestrial mammals, density of
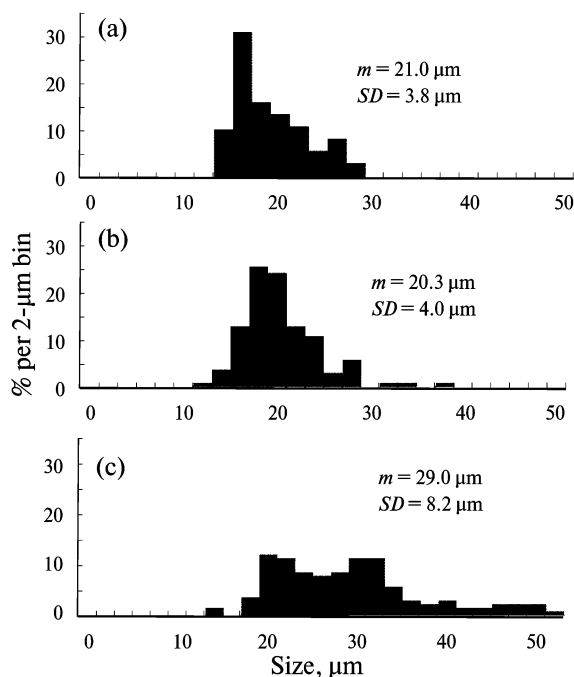
Fig. 4. Distributions of ganglion cell sizes. (a) Nasal area of cell concentration, (b) temporal area of cell concentration, (c) retinal periphery with low cell density. m—Mean value, SD—standard deviation.

ganglion cells. The low density was also reported in other cetaceans. The maximum density of retinal ganglion cells in the rough-toothed dolphin revealed in this study (on average 594 cells/mm^2 for two wholemounts) is comparable to the values (500–700 cells/mm^2) in other dolphin species: the bottlenose dolphin *T. truncatus* [2, 26] and the Dall's porpoise *Phocoenoides dalli* [27]. Among all cetaceans inhabiting transparent seawater, the lowest density ($\leq$ 330 cells/mm^2) was found in the retina of the killer whale *O. orca* [5].

Thus, the density of ganglion cells in the retina of the rough-toothed dolphin is comparable to those in other toothed whales. This density in toothed cetaceans, including the rough-toothed dolphin, is one order of magnitude lower compared to terrestrial predators in which it varies from 7000 to 14000 cells/mm^2 [14, 28, 29].

Topography of ganglion cell distribution. In this study, we revealed two areas of increased density of ganglion cells in the retina of the rough-toothed dolphin. An analogous topography of ganglion cells that form areas of maximum cell density not in the center but at the periphery of the retina is characteristic of many cetacean spe-

cies: bottlenose dolphin *T. truncatus* [2], common dolphin *D. delphis* [30], Dall's porpoise *Ph. Dalli* [31], false killer whale *P. crassidens* [6], beluga whale *D. leucas* [4, 6], Chinese river dolphin *Lipotes vexillifer*, Indo-Pacific finless porpoise *Nephocaena phocaenoides* [32], gray dolphin (tucuxi) *Sotalia fluviatilis* [3]. The only exception is the Amazon river dolphin *Inia geoffrensis* inhabiting turbid waters under conditions of low luminance. This species has only a single area of increased ganglion cell density located in the ventral retinal area and projecting to the upper visual field quadrant where illuminance is higher [9].

The possible functional significance of these two areas of increased ganglion cell density was considered previously in relation with the dolphin's ability to use different retinal areas to view objects both in water and air [2]. The two areas correlate with the pupil shape in cetaceans in which the upper margin of the iris forms a protrusion (operculum) which shields the lens. When the pupil constricts, the operculum moves downward so that the pupil acquires a characteristic U-like shape, while in the case of considerable protrusion, the pupil turns into two slit apertures located in its temporal and nasal parts [33−35]. These apertures are situated opposite to the retinal areas of increased ganglion cell density in the temporal and nasal retinal areas. As a result, light projects on the areas of increased ganglion cell density, passing through the peripheral corneal areas, then through the slit apertures of the pupil, and finally through the spherical lens. At high illuminance, which is characteristic of air vision, light reaches the retina through the peripheral part of the cornea having a far lower curvature compared to the rest of the corneal surface. Due to a lower curvature of the corneal periphery, myopia is reduced, and an emmetropic "optical window" forms in air [11, 36, 37]. In this case, the temporal zone of the retina is used, which provides frontal vision and, probably, binocular vision [38]. At low illuminance (which is often the case under water), light enters the eye through the dilated (mydriatic) pupil and falls on all areas of increased ganglion cell density, thus providing a wide field of monocular vision. However, in this case, the corneal curvature does not generate myopia since the refraction indices before the cornea (water) and

behind it (fluid in the anterior chamber) are practically the same. Due to such a combination of the optical system of the eye and the retinal organization, cetaceans have virtually emmetropic vision both in water and air.

Retinal resolution. This characteristic of the retina can be defined as an average angular distance between adjacent ganglion cells. The average linear distance can be derived from data on the distribution density of ganglion cells by a straightforward calculation:

$$L = \sqrt{D}, \qquad (1)$$

where L (mm)—distance and D (cells/mm^2)—cell density. To convert a linear distance into angular, it is necessary to know the distance from the posterior nodal point of the optical system to the retina (posteronodal distance):

$$\alpha = 180L/\pi r = 180/\pi r \sqrt{D}, \qquad (2)$$

where α (deg)—angular distance between cells, and r (mm)—posteronodal distance. The D values was obtained in the present study, while the posteronodal distance r was not measured here due to a paucity of the available material. As a first approximation, one can proceed from the fact that the dolphin's optical system is centrally symmetrical, with the center of the system being a common point of the center of the lens and the center of the retinal hemisphere. Since in water the cornea does not function as a light-refracting element, the only light-refracting element must be an almost spherical lens. In this case, the only nodal point of the optical system coincides with the center of the lens and hence with the center of the retinal hemisphere, while the posteronodal distance is equal to the radius of the retinal hemisphere. At the eyecup diameter (an average value between vertical and horizontal diameters) of 25.5 mm, the posteronodal distance can be taken equal to 12.75 mm. This value is an approximate assessment based on a series of assumptions; however it can be used to assess retinal resolution at the first approximation. By substituting into the expression (2) the average value of ganglion cell density in the areas of their maximum concentration (594 cells/mm^2) and the accepted value of the posteronodal distance (12.75 mm), we obtain $\alpha = 0.18° = 11'$. This value is close to the assessments of retinal resolution

Table 1. Retinal resolution in some cetaceans

Species	Retinal resolution, angular min	Ref
Marine dolphins		
Common dolphin	8	[30]
Bottlenosed dolphin	9	[2]
	8	[34]
Dall's porpoise	11.5	[31]
False killer whale	9.3	[6]
Pacific white-sided dolphin	11.2	[6]
Beluga whale	11.8	[6]
	14.4	[4]
Killer whale	9.6	[5]
River dolphins		
Tucuxi	25	[3]
Amazon river dolphin	40	[9]
True whales		
Gray whale	11	[7]
Bryde's fin whale	6.3*	[8]
Hump-backed whale	9.1*	[8]
This study		
Rough-toothed dolphin	11	

Retinal resolution data as calculated by the ganglion cell density for the aqueous medium (corneal light refraction disregarded). Data marked by asterisk (*) expressed by the authors in cycle/degree and recalculated into an angular resolution, accepting that angular resolution is equal to half a cycle, i.e. $R = 60/2F$, where R—resolution in angular minutes and F—resolution in cycle/degree, while the multiplier 60 converts the resultant values of retinal resolution from degrees into minutes.

obtained in other toothed whales (both Delphinidae and other families) inhabiting transparent ocean waters (Table 1).

CONCLUSION

The topography of the ganglion layer and retinal resolution in the rough-toothed dolphin are basically similar to those in other toothed cetaceans inhabiting ocean waters. Peculiarities of the habitat of this species (both low-transparency coastal waters and high-transparency ocean waters) are not reflected in the organization of their retina.

ACKNOWLEDGMENTS

AUTHORS' CONTRIBUTION

A.M. Mass: task formulation, processing of the material, examination of preparations, writing a manuscript. A.Ya. Supin: data processing software, quantitative data analysis, writing a manuscript.

FUNDING

COMPLIANCE WITH ETHICAL STANDARDS

All applicable international, national and institutional principles of handling and using experimental animals for scientific purposes were observed.

This study did not involve human subjects as research objects.

CONFLICT OF INTEREST

Authors of this study have no conflict of interest.

REFERENCES

1. Mass, A.M. and Supin, A.Ya., Adaptive features of aquatic mammal's eye, *Anat. Rec.*, 2007, vol. 290, pp. 701–715.

2. Mass, A.M. and Supin, A.Ya., Ganglion cells topography of the retina in the bottlenosed dolphin, *Tursiops truncates*, *Brain Behav. Evol.*, 1995, vol. 45, pp. 257–265.

3. Mass, A.M. and Supin, A.Ya., Retinal topography and visual acuity in the riverine tucuxi, (*Sotalia fluviatilis*), *Marine Mammal Sci.*, 1999, vol. 15, pp. 351–365.

4. Mass, A.M. and Supin, A.Ya., Visual field organization and retinal resolution of the beluga, *Delphinapterus leucas* (Pallas), *Aquatic Mammals*, 2002, vol. 28, pp. 241–250.

5. Mass, A.M., Supin, A.Y., Abramov, A.V., Mukhametov, L.M., and Rozanova, E.I., Ocular anatomy, ganglion cell distribution, and retinal resolution of a killer whale (*Orcinus orca*), *Brain Behav. Evol.*, 2013, vol. 81, pp. 1–11.

6. Murayama, T. and Somiya, H., Distribution of ganglion cells and object localizing ability in the retina of three cetaceans, *Fisheries Sci.*, 1998, vol. 64, pp. 27–30.

7. Mass, A.M. and Supin, A.Ya., Ocular anatomy, retinal ganglion cell distribution, and visual resolution in the gray whale, *Eschrichtius gibbosus*, *Aquatic Mammals*, 1997, vol. 23, pp. 17–28.

8. Lisney, T.J. and Collin, S.P., Retinal topography in two species of ballen whale (Cetacea: Mysticety), *Brain Behav. Evol.*, 2018, vol. 92, pp. 97–116.

9. Mass, A.M. and Supin, A.Ya., Distribution of ganglion cells in the retina of an Amazon river dolphin, *Inia geoffrensis*, *Aquatic Mammals*, 1989, vol. 15, pp. 49–56.

10. West, K.L., Mead, J.G., and White, W., Mammalian sciences *Steno bredanensis* (Cetacea: Delphinidae), *Mammalian Species. American Society of Mammologists*, 2011, vol. 43(886), pp. 177–189.

11. Dral, A.D.G., Problems in image-focusing and astigmatism in cetacea – a state of affairs, *Aquatic Mammals*, 1974, vol. 2, pp. 22–28.

12. Stone, J., *The Wholemount Handbook. A Guide to the Preparation and Analysis of Retinal Wholemounts*, Maitland, Sidney, 1981.

13. Ullmann, J.F.P., Moore, B.A., Templ, S.E., Fernandez-Juricic, E., and Collin, S.P., The retinal wholemount technique: a window to understanding the brain and behavior, *Brain, Behav. Evol.*, 2012, vol. 79, pp. 26–44.

14. Peichl, L., Topography of ganglion cells in the dog and wolf retina, *J. Comp. Neurol.*, 1992, vol. 324, pp. 603–620.

15. Mass, A.M. and Supin, A.Y., Retinal ganglion cell layer of the Caspian seal *Pusa capsica*: Topography and localization of the high-resolution area, *Brain Behav. Evol.*, 2010, vol. 76, pp. 144–153.

16. Hanke, F.D., Peichl, L., and Dehnhardt, G., Retinal ganglion cell topography in juvenile harbor seals (*Phoca vitulina*), *Brain, Behav. Evol.*, 2009, vol. 74, pp. 102–109.

17. Hughes, A., Population magnitudes and distribution of the major modal classes of cat retinal ganglion cells as estimated from HRP filling and systematic survey of the soma diameter spectra for classical neurons, *J. Comp. Neurol.*, 1981, vol. 197, pp. 303–339.

18. Wong, R.O.L., Wye-Dvorak, J., and

Henry, G.H., Morphology and distribution of neurons in the retina ganglion cell layer of the adult Tammar wallaby *Macropus eugenii*, *J. Comp. Neurol.*, 1986, vol. 253, pp. 1−12.

19. Wässle, H., Hoon, C.M., and Muller, F., Amacrine cells in the ganglion cell layer of the cat retina, *J. Comp. Neurol.*, 1987, vol. 265, pp. 391−408.

20. Wong, R.O.L. and Hughes, A., The morphology, number and distribution of a large population of confirmed displaced amacrine cells in the adult cat retina, *J. Comp. Neurol.*, 1987, vol. 255, pp. 159−177.

21. Dawson, W.W. and Perez, J.M., Unusual retinal cells in the dolphin eye, *Science*, 1973, vol. 181, pp. 747−749.

22. Dawson, W.W., Hawthorne, M.N., Jenkins, R.L., and Goldston, R.T., Giant neural system in the inner retina and optic nerve of small whales, *J. Comp. Neurol.*, 1982, vol. 205, pp. 1−7.

23. Pütter, A., Die Augen der Wassersaugetierre, *Zool. Jahrb. Abth. Anat. Ontog. Thiere*, 1903, vol. 17, pp. 99−402.

24. Jacobs, M.S., Further fiber counts of cetacean cranial nerve, *Anat. Rec.*, 1973, vol. 175, pp. 505–506.

25. Morgane, P.J. and Jacobs, M.S., Comparative anatomy of the cetacean nervous system, *Functional Anatomy of Marine Mammals*, Harrison, R.J., Ed., New York, Academic Press, 1972, pp. 117−244.

26. Dral, A.D.G., On the retinal anatomy of Cetacea (mainly *Tursiops truncatus*), Functional Anatomy of Marine Mammals, Harrison, R.J., Ed., London, Academic Press, 1977, vol. 3, pp. 81−134.

27. Murayama, T., Fujise, Y., Aoki, I., and Ishii, T., Histological characteristics and distribution of ganglion cells in the retina of the Dall's porpoise and minke whale, *Marine Mammal Sensory Systems*, Thomas, J.A., Kastelein, R.A., and Supin, A.Ya., Eds., New York, Plenum, 1992, pp. 137−145.

28. Stone, J., The number and distribution of ganglion cells in the cat's retina, *J. Comp. Neurol.*, 1978, vol. 180, pp. 753−772.

29. Calderone, J.B., Reese, B.E., and Jacobs, G.H., Topography of photoreceptors and retinal ganglion cells in the spotted hyena (*Crocuta crocuta*), *Brain Behav. Evol.*, 2003, vol. 62, pp. 182−192.

30. Dral, A.D.G., The retinal ganglion cells of *Delphinus delphis* and their distribution, *Aquatic Mammals*, 1983, vol. 10, pp. 57−68.

31. Murayama, T., Somiya, H., Aoki, I., and Ishii, T., Retinal ganglion cell size and distribution predict visual capabilities of Dall's porpoise, *Marine Mammal Sci.*, 1995, vol. 11, pp. 136−149.

32. Gao, A. and Zhou, K., On the retinal ganglion cells of Neophocoena and Lipotes, *Acta Zool. Sin.*, 1987, vol. 33, pp. 316−332.

33. Rochon-Duvigneaud, A., L'oeil des Cétacés, *Archives Museum National Histoire Naturelle Paris*, 16, 1939.

34. Herman, L.M., Peacock, M.F., Yunker, M.P., and Madsen, C.J., Bottlenosed dolphin: Double-slit pupil yields equivalent aerial and under water diurnal acuity, *Science*, 1975, vol. 189, pp. 650−652.

35. Dawson, W.W., Adams, C.K., Barris, M.C., and Litzkov, C.A., Static and kinetic properties of the dolphin pupil, *Am. J. Physiol.*, 1979, vol. 237, pp. R301−R305.

36. Dral, A.D.G., Aquatic and aerial vision in the bottle-nosed dolphin, *Neth. J. Sea Res.*, 1972, vol. 5, pp. 510−513.

37. Dawson, W.W., Schroeder, J.P., and Sharpe, S.N., Corneal surface properties of two marine mammal species, *Marine Mammal Sci.*, 1987, vol. 3, pp. 186−197.

38. Dawson, W.W., The Cetacean Eye, *Cetacean Behavior: Mechanisms and Functions*, Herman, L.M., Ed., New York, Willey, 1980, pp. 53−100.

Translated by A. Polyanovsky